



## Get Clarity On Generics

Cost-Effective CT & MRI Contrast Agents



FRESENIUS  
KABI

WATCH VIDEO

# AJNR

### **Imaging studies in a unique familial dysmyelinating disorder.**

K W Gripp, R A Zimmerman, Z J Wang, L B Rorke, A C Duhaime, L Schut, P T Molloy, S H Tucker, E H Zackai and M Muenke

This information is current as  
of August 18, 2025.

*AJNR Am J Neuroradiol* 1998, 19 (7) 1368-1372

<http://www.ajnr.org/content/19/7/1368>

## Imaging Studies in a Unique Familial Dysmyelinating Disorder

Karen W. Gripp, Robert A. Zimmerman, Zhiyue J. Wang, Lucy B. Rorke, Ann-Christine Duhaime, Luis Schut, Patricia T. Molloy, Samuel H. Tucker, Elaine H. Zackai, and Maximilian Muenke

**Summary:** We report the imaging findings in five patients with a unique dysmyelinating disorder. MR studies of these infants showed obstructive hydrocephalus caused by mass effect produced by an enlarged cerebellum. The white matter of an enlarged cerebrum and cerebellum showed delayed myelination. Proton spectroscopy showed normal *N*-acetylaspartate (NAA) levels. While the dysmyelinating disorder was clearly differentiated from Canavan disease by an absence of elevated NAA and differing histopathologic findings and autosomal-dominant inheritance pattern, there were similarities to this disease in the presentation and, to some extent, in the initial imaging findings.

Although white matter abnormalities in infants can be of diverse origin, familial cases are almost always due to a form of leukodystrophy. These are autosomal-recessive inherited disorders, except for the X-linked adrenoleukodystrophy, Pelizaeus-Merzbacher disease, and encephalopathies caused by mitochondrial DNA abnormalities. We describe five cases of a previously unreported autosomal-dominant white matter abnormality that presented in infancy with macrocephaly.

### Case Reports

#### Case 1

The proband was the son of nonconsanguineous Ashkenazi Jewish parents. His birth measurements were unremarkable. By age 5 months he had rotatory nystagmus, spasticity, and an increased head circumference (>98%). A ventriculogram showed obstruction at the fourth ventricle. Surgical exploration revealed an enlarged cerebellum causing obstructive hydrocephalus. At cerebellar biopsy, the white matter was spongy and myelin granules were seen in enlarged oligodendrocytes. Ultrastructural analysis identified the cytoplasmic granules as myelin sheath precursors. A frontal lobe biopsy revealed similar findings. The patient's development improved after shunt placement, and spasticity decreased; however, diplegia and nystagmus persisted. At 13 years, his IQ was >40 (Wechsler Intelligence scale for Children–Revised). A brain MR study at

age 13 showed atrophy with enlargement of the lateral ventricles, dilatation of the sulci, and evidence of myelin formation on T1-weighted images. T2-weighted images showed some hypointense myelin formation, but with high signal intensity present diffusely (Fig 1). The internal capsules and portions of the basal ganglia also showed increased signal intensity. At present (age 22 years), his head circumference measures 62 cm (>98%), his speech is extremely slow but clear, he uses a wheelchair, and works under supervision. There has been no regression at any time.

Previously performed funduscopy revealed slightly pale optic disks. Nerve conduction studies and EMG were normal; assays for arylsulfatase A, very long chain fatty acids, phytanic acid, and urine for metabolic screening were normal.

#### Case 2

The proband's sister had a normal head circumference at birth but macrocephaly developed in infancy. A pneumoencephalogram showed a "large brain" without hydrocephalus. Her intellectual development was normal, but motor development was described as slow. On brain MR studies performed at age 22 years, extensive supra- and infratentorial atrophy was noted, with changes involving the cerebellar folia. The cerebral and cerebellar white matter appeared myelinated on T1-weighted images (Fig 2); however, there was increased signal intensity of the white matter on T2-weighted studies. The lateral ventricles were dilated as a result of volume loss.

Currently, at age 26 years, the patient's head circumference is 60 cm (>98%); her tone is normal, Babinski response is absent, and there is no clonus. Gait and speech are normal.

#### Case 3

This patient is the daughter of the woman in case 2 and a nonconsanguineous, non-Ashkenazi partner. Her head circumference was normal at birth, but increased to >98% at 5 months. An MR study obtained at 10 months showed obstruction of the aqueduct of Sylvius, which was kinked forward by mass effect from the cerebellum. The cerebellar white matter appeared unmyelinated on both T1- and T2-weighted images; that is, hypointense on T1-weighted images and hyperintense on T2-weighted images (Fig 3B). All cerebellar folia appeared expanded and the sulci were compressed (Fig 3A). The brain stem was not expanded, although there was evidence of unmyelinated portions on T2-weighted images in the midbrain and

Received April 24, 1997; accepted after revision October 6.

K.W.G. is supported by the Howard Hughes Medical Institute.

From the Division of Human Genetics and Molecular Biology (K.W.G., E.H.Z., M.M.), the Department of Radiology (R.A.Z., Z.J.W.), the Department of Anatomic Pathology (L.B.R.), the Division of Neurosurgery (A-C.D., L.S.), and the Division of Neurology (P.T.M., S.H.T.), The Children's Hospital of Philadelphia.

Address reprint requests to Maximilian Muenke, MD, The Children's Hospital of Philadelphia, Division of Human Genetics and Molecular Biology, 34th and Civic Center Blvd, Philadelphia, PA 19104.

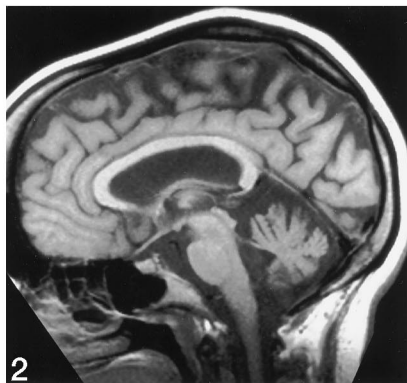
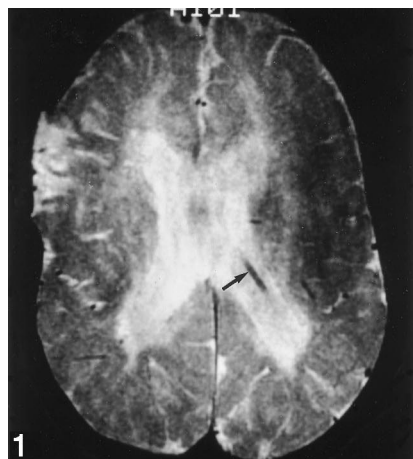


FIG 1. Case 1: age 13 years. Axial T2-weighted MR image (2000/80/2) shows dilated lateral ventricles, a shunt within the left lateral ventricle (arrow), and abnormally increased signal in the white matter surrounding both lateral ventricles.

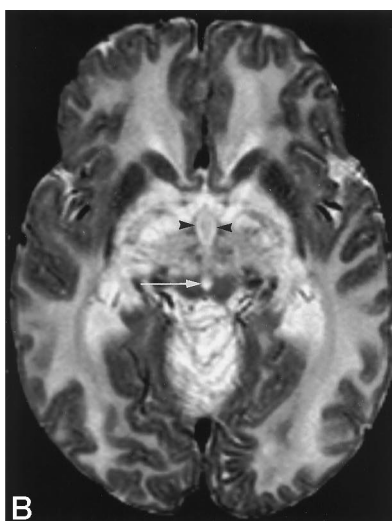
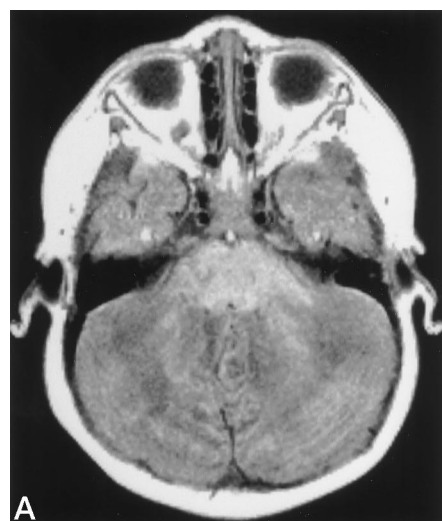


FIG 2. Case 2: age 23 years. Sagittal T1-weighted MR image (660/14/1) shows the lateral ventricles to be dilated, the corpus callosum to be myelinated, and the cerebellum to be atrophic.

FIG 3. Case 3: age 8 months.

A, Axial T1-weighted MR image (600/15/1) at the level of the cerebellar hemispheres and pons shows both cerebellar hemispheres to be expanded, the white matter to be hypointense, and the pons and fourth ventricle to be compressed.

B, Axial T2-weighted MR image (3000/80/1) at the level of the midbrain shows the central midbrain and adjacent thalami and basal ganglia to be hyperintense. The white matter of the frontal, temporal, and occipital lobes is also hyperintense, but not to the same extent as the cerebellar vermis, thalami, brain stem, and internal capsules. The aqueduct of Sylvius is dilated (arrow), as is the anterior third ventricle (arrowheads).

pons. There was no evidence of myelination in the corpus callosum. Decreased myelination of the centrum ovale was indicated by increased signal intensity on T2-weighted images from the subcortical U fibers down to the periependymal tissues. The optic chiasm and the optic nerves were enlarged and hypointense on T1-weighted images, lacking normal myelination. The posterior limbs, genu, and, to a much lesser extent, the anterior limbs of the internal capsules also had low signal on T1-weighted images, indicating decreased myelination. The posterior limbs and the genu of the internal capsule were markedly expanded, with abnormal white matter signal intensity on T2-weighted images projecting into and extensively involving the globus pallidus. The putamina and caudates appeared relatively spared, having a more normal appearance. Proton MR spectroscopy showed normal *N*-acetylaspartate (NAA).

At present (age 5 years), with the exception of persistent hydrocephalus requiring a ventriculoperitoneal shunt, growth and development have continued appropriately for age. Neurologic examination showed normal tone, but with symmetrically increased deep tendon reflexes and sustained clonus at the right ankle. Babinski response is present bilaterally. Speech and gait are normal. Studies yielding normal results include lysosomal enzymes in white cells and serum, plasma amino acids, urine organic acids, and mucopolysaccharides in urine.

#### Case 4

This patient is the brother of the girl in case 3, born after the birth of another, apparently unaffected, girl. Although birth

measurements were normal, head circumference increased to 61.5 cm (>98% for adults) at 5 months. Central tone was decreased with normal peripheral tone and symmetrical deep tendon reflexes, without clonus or Babinski response. He was unable to roll over and did not fix or follow. Nystagmus was present.

A brain MR study at 5½ months showed findings similar to his sister's, including obstructive hydrocephalus due to cerebellar enlargement (Fig 4). Proton spectroscopy showed decreased NAA and creatine (Cr) (Table 1). A ventriculoperitoneal shunt was placed. An MR study at 11 months showed anterior and upward expansion and displacement of the brain stem, in part caused by marked cerebellar enlargement. At 1 year he improved slightly in his ability to fix and follow, but had little head control and remained macrocephalic. Findings on fundoscopic examination, electroretinography, and chromosomal studies were normal.

#### Case 5

The proband's father had normal intelligence and no neurologic abnormalities. Head circumference was 60 cm (>98%). His mother's head circumference was reportedly enlarged. An MR examination at age 54 years showed ventricle size at the upper limit of normal and prominent sulci without cerebellar atrophy. Myelination appeared normal on T1-weighted images, but there was some diffuse increase in signal intensity on T2-weighted images (Fig 5). Proton spectroscopy showed normal NAA (Table 1) and decreased Cr in the cerebral hemispheres.

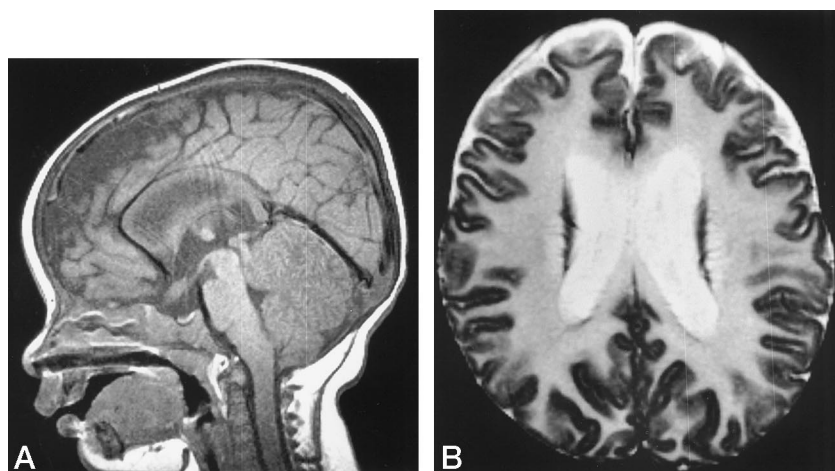


FIG 4. Case 4: age 5 months.

A, Sagittal T1-weighted MR image (700/14/1) shows hypointense white matter expanding the cerebellum, producing mass effect with forward displacement of the superior medullary velum and superior vermis against the inferior collicular plate and cerebral aqueduct. This produces relative obstruction of CSF flow at the aqueductal level. The optic chiasm and corpus callosum are enlarged but hypointense. The third and lateral ventricles are dilated.

B, Axial T2-weighted MR image (3000/120/1) at the level of the body of the lateral ventricles shows all white matter to be hyperintense.

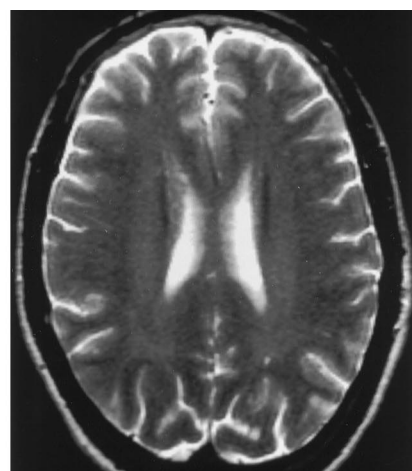


FIG 5. Case 5: age 54 years.

Axial T2-weighted MR image (3500/93/1) at the level of the body of the lateral ventricles shows mild ventricular enlargement, as well as sulcal prominence. The white matter shows a diffuse, hazy, increased signal intensity, but appears to be myelinated.

#### MR Imaging and Proton MR Spectroscopic Studies

Table 2 summarizes the MR findings of our two patients during infancy in respect to white matter disease and contrasts it with similar findings in five infants with known Canavan disease.

MR proton spectroscopy was performed in cases 3, 4, and 5 using a single-voxel stimulated-echo acquisition mode (STEAM) sequence. For comparison with the spectroscopic findings in the two infants reported in this series, the two patients with Canavan disease closest in age were chosen. Control spectra from patients without known neurologic CNS disease affecting the brain served as control subjects. For the adult patient in this series, case 5, adult control subjects were selected (Table 1).

For case 3, the NAA/Cr ratio was almost normal (data not shown). Case 4 had a decreased NAA level and case 5 had a normal NAA level, while for those with Canavan disease, the NAA/Cr ratio and the NAA level were highly elevated. The

choline (Cho)/Cr ratio in patient 3 was normal, as were the Cho levels in cases 4 and 5.

#### Discussion

The sequence in which abnormalities appear on imaging studies in this primary dysmyelinating disorder is illustrated by the findings in cases 3 and 4 in infancy, which show supra- and infratentorial lack of myelination and white matter expansion, that evolve to the findings seen in cases 1 and 2 during adolescence and adulthood. These consist of abnormal myelination on T2-weighted images and supra- and infratentorial atrophy. The imaging studies of cases 3 and 4, obtained during infancy, showed almost identical findings of obstructive hydrocephalus from com-

TABLE 1: Proton MR spectroscopic findings in cases 4 and 5\*

	Basal Ganglion			Cerebral Hemispheres		
	Cho	Cr	NAA	Cho	Cr	NAA
Case 4 (age 6 mo)†	0.9	3.7	3.5	0.8	3.6	3.2
Case 5 (age 54 y)†	0.52	5.2	6.1	0.7	3.5	6.1
Patient with Canavan disease (age 8 mo)	0.4	4.0	8.8	0.5	2.3	6.7
Control subject (mean ± SD)‡	0.73 ± 0.15	5.5 ± 0.6	5.8 ± 0.6			
Control subject (age 8 mo)				0.8	4.7	5.8
Control subject (mean ± SD)§				0.7 ± 0.2	4.9 ± 1.1	6.0 ± 0.3

\* Data in case 3 were obtained only as ratios, not shown here.

† The proton MR spectrum was acquired using a stimulated-echo acquisition mode (STEAM) sequence with parameters of 1600/20 (TR/TE), TM (middle time) = 30, and a voxel size of  $2 \times 2 \times 2 \text{ cm}^3$  (values are in units of mmol per voxel volume without correcting for T1 saturation effects).

‡ Based on Lam et al (14).

§ Our data on five adult control subjects.



**TABLE 2: Summary of MR findings of signal intensity and volume during infancy**

	Primary Dysmyelination		Canavan Disease	
	T1	T2	T1	T2
Brain stem				
Basis pontis	N	A	N	N
Other	N	A	A	A
Cerebellum				
Middle cerebellar peduncle	A	A	N	N
Deep cerebellar white matter	A	A	A	A
Internal capsules	A	A	A	A
Corpus callosum	A	Too young, A expected	A	A
Subcortical white matter	A $\times$ 1, others too young	Too young	S	A $\times$ 3, other too young
Optic nerves and chiasm	A	A	N	N
Basal ganglia				
Caudate and putamina	N	N	N	N
Globus pallidi	A	A	N	N
Volume				
Cerebellum	+		N	
Cerebrum	+		+	
Lateral ventricles	+		N	
Optic chiasm	+		—	

Note.—N indicates normal signal intensity for age; A, abnormal signal intensity for age; +, increased volume of tissue; N, normal volume; —, decreased volume of tissue.

pression of the aqueduct and the fourth ventricle by expanded abnormal cerebellar tissue. The white matter of both cerebrum and cerebellum was grossly abnormal with respect to myelination and volume (Figs 3 and 4). While patient 3 had normal intellectual development after shunt placement, patient 4 had severe neurologic impairment unresolved by shunt placement. Subsequent studies of the brain in patient 4 showed worsening of the white matter enlargement, causing anterior displacement of the brain stem.

Although imaging studies of equal quality were unavailable for the proband at infancy, he also had obstructive hydrocephalus due to cerebellar mass effect. However, an MR study performed in adolescence showed cerebral (Fig 1) and cerebellar atrophy. While the white matter appeared myelinated on T1-weighted images, there was diffuse high signal intensity on T2-weighted images within the supra- (Fig 1) and infratentorial white matter. These findings are similar to those noted on an adult MR study of the proband's sister (Fig 2), who is the mother of patients 3 and 4. Although she never incurred obstructive hydrocephalus, her cerebellum was clearly affected by white matter changes and atrophy. Thus, the presence or absence of obstructive hydrocephalus appears to be a quantitative difference, caused by the severity of

cerebellar enlargement, rather than a qualitative difference. The father of patients 1 and 2 (case 5) had subtle findings of white matter abnormality and possibly mild supratentorial atrophy on an MR study obtained at age 54 years (Fig 5). While the abnormalities in this patient are subtle, the presence of macrocephaly suggests that a similar process of cerebral enlargement and delayed myelination had occurred during infancy, later giving way to abnormal myelination and atrophy. This process also affects the optic chiasm, which were enlarged in the infants and small in the adults.

White matter abnormalities in infants may be of diverse origin, among which are a variety of leukodystrophies. These are autosomal-recessive inherited disorders, except for the X-linked adrenoleukodystrophy, Pelizaeus-Merzbacher disease, and encephalopathies caused by mitochondrial DNA abnormalities. Progressive deterioration is characteristic of patients with these disorders (1). The nonprogressive course seen in our patients is thus different from previously described leukodystrophies.

Proton MR spectroscopy is used to obtain information about brain tissue metabolism. A decrease in the NAA/Cr ratio or the NAA level is an almost universal finding in all leukodystrophies and demyelinating disorders, including adrenoleukodystrophy (2, 3), metachromatic leukodystrophy (4, 5), and multiple sclerosis (6, 7), except for Canavan disease (5, 8–10), in which the NAA level or NAA/Cr ratio is increased. NAA is present only in neuronal cells, and a decrease in NAA in degenerative white matter diseases is consistent with shrinkage and loss of neuronal cells. Accumulation of NAA despite tissue degeneration is unique in Canavan disease, which is caused by a deficiency of aspartoacylase, an enzyme in the NAA catabolic pathway. Normal levels of NAA have also been observed in late-onset Pelizaeus-Merzbacher disease (11). There was no increase in NAA level or NAA/Cr ratio in the three patients reported here in whom proton MR spectroscopy was performed. In fact, all three patients had normal or mildly decreased NAA or NAA/Cr, consistent with a mild form of a leukodystrophy. Cho or Cho/Cr levels in white matter disorders are variable. They may be increased in adrenoleukodystrophy (2, 3), early-onset Pelizaeus-Merzbacher disease (11), and multiple sclerosis (6, 7). This is thought to reflect an increased membrane turnover. In many other disorders (11, 12), including Canavan disease (5, 8–10), Cho levels or Cho/Cr ratios are decreased, consistent with decreased membrane constituents in the brain tissue. The three patients all had a Cho level or Cho/Cr ratio in the normal range, higher than that found in Canavan disease. The nearly normal Cho level in a leukodystrophy suggests relatively little brain tissue damage or, alternatively, tissue damage that is balanced by increased membrane turnover. In these patients it is more likely that the former is the case.

Comparison of the two infants with this unique dysmyelinating disorder with the five infants who had Canavan disease yielded both similarities and differ-

ences. Both groups showed similar abnormalities of signal intensity on T1- and T2-weighted images of the deep cerebellar white matter, internal capsule, corpus callosum, and subcortical white matter; although two of the patients with Canavan and the infants with the primary dysmyelinating disease were too young to expect full myelination of cerebral white matter. The white matter was abnormally hypointense on T1-weighted images and hyperintense on T2-weighted images in the subcortical white matter and corpus callosum. Significant differences between the groups were found in the brain stem. The basis pontis was normal in the patients with Canavan disease, while the rest of the brain stem was abnormal. In the patients with primary dysmyelination, the brain stem was normal on T1-weighted images and abnormal on T2-weighted images. Changes noted only in the patients with primary dysmyelination affected the optic chiasm and the globus pallidi. The volume increase of the cerebellum, the optic chiasm, and the lateral ventricles was also seen only in this new disorder. Both groups showed enlargement of the cerebrum. However, while patients with Canavan disease develop megaloccephaly because of excessive water, they do not present with obstructive hydrocephalus from mass effect. Ventricular enlargement in Canavan disease can occur secondary to atrophy, but this is generally seen later, at age 2 to 4 years. Proton MR spectroscopy has been applied by many investigators to the study of Canavan disease (5, 8–11), in which the NAA level and NAA/Cr ratio are markedly elevated and the Cho level and Cho/Cr or Cho/NAA ratios are decreased. The diagnosis of Canavan disease is based on the increased NAA levels found in brain and urine (13). These changes were not present in our patients with the newly reported primary dysmyelinating disorder.

### Conclusion

Because patients with Canavan disease can exhibit developmental arrest and macrocephaly, similar to our patients, this unique dysmyelinating disorder should be considered when the presumptive diagnosis of Canavan disease cannot be confirmed. For diagnostic purposes, the most significant difference is that this newly described disorder lacks the elevated NAA level and decreased Cho level characteristic of Canavan disease. In addition, the obstructive hydrocephalus caused by cerebellar enlargement seen in our patients does not occur in Canavan disease or other leukodystrophies. On histologic examination, the

white matter of our proband appeared spongy, similar to findings seen in leukodystrophies, such as Canavan disease; however, the oligodendrocytic inclusion bodies consisting of myelin sheath precursors are unique to this dysmyelinating disorder. Since there is male-to-male transmission, the inheritance pattern in this family is most consistent with autosomal-dominant inheritance and inconsistent with maternal inheritance. This disorder can thus be differentiated from previously described leukodystrophies on the basis of findings at MR imaging and MR spectroscopy, inheritance pattern, and histopathologic findings.

### References

1. Aicardi J. **The inherited leukodystrophies: a clinical overview.** *J Inher Metab Dis* 1993;16:733–743
2. Tzika AA, Ball WSJ, Vigneron DB, Dunn RS, Nelson SJ, Kirks DR. **Childhood adrenoleukodystrophy: assessment with proton MR spectroscopy.** *Radiology* 1993;189:467–480
3. Kruse B, Barker PB, van Zijl PC, Duyn JH, Moonen CT, Moser HW. **Multislice proton magnetic resonance spectroscopic imaging in X-linked adrenoleukodystrophy.** *Ann Neurol* 1994;36:595–608
4. Kruse B, Hanefeld F, Christen HJ, et al. **Alterations of brain metabolites in metachromatic leukodystrophy as detected by localized proton magnetic resonance spectroscopy in vivo.** *J Neurol* 1993;241:68–74
5. Wang Z, Zimmerman RA, Sauter R. **Proton MR spectroscopy of the brain: clinically useful information obtained in assessing CNS diseases in children.** *AJR Am J Roentgenol* 1996;167:191–199
6. Matthews PM, Francis G, Antel J, Arnold DL. **Proton magnetic resonance spectroscopy for metabolic characterization of plaques in multiple sclerosis.** *Neurology* 1991;41:1251–1256
7. Bruhn H, Frahm J, Merboldt KD, et al. **Multiple sclerosis in children: cerebral metabolic alterations monitored by localized proton magnetic resonance spectroscopy in vivo.** *Ann Neurol* 1992;32:140–150
8. Grodd W, Krageloh-Mann I, Petersen D, Trefz FK, Harzer K. **In vivo assessment of N-acetylaspartate in brain in spongy degeneration (Canavan's disease) by proton spectroscopy.** *Lancet* 1990;336:437–438
9. Marks HG, Caro PA, Wang ZY, et al. **Use of computed tomography, magnetic resonance imaging, and localized 1H magnetic resonance spectroscopy in Canavan's disease: a case report.** *Ann Neurol* 1991;30:106–110
10. Barker PB, Bryan RN, Kumar AJ, Naidu S. **Proton NMR spectroscopy of Canavan's disease.** *Neuropediatrics* 1992;23:263–267
11. Grodd W, Krageloh-Mann I, Klose U, Sauter R. **Metabolic and destructive brain disorders in children: findings with localized proton MR spectroscopy.** *Radiology* 1991;181:173–181
12. van der Knaap MS, van der Grond J, Luyten PR, den Hollander JA, Nauta JJ, Valk J. **1H and 31P magnetic resonance spectroscopy of the brain in degenerative cerebral disorders.** *Ann Neurol* 1992;31:202–211
13. Matalon R, Michals K, Sebasta D, Deanching M, Gashkoff P, Casanova J. **Aspartoacylase deficiency and N-acetylaspartic aciduria in patients with Canavan's disease.** *Am J Med Genet* 1988;29:463–471
14. Lam W, Wang Z, Zhao H, et al. **1H MR spectroscopy of the pediatric basal ganglia, a semiquantitative analysis.** *Neuroradiology* (in press)